Development of High-Gradient Dielectric Laser-Driven Particle Accelerator Structures

Ref: Stanford University
Grant No. DE-FG06-97ER41276

Final Report

Submitted to:
Division of High Energy Research
Technical Program Manager Contact: Michael Zisman
Office of Energy Research
Department of Energy

Submitted by:

Robert L. Byer, Principal Investigator
Professor of Applied Physics
Edward L. Ginzton Laboratory
Stanford University
Stanford, CA. 94305-4085
Tel. 650-723-0226
Email: byer@stanford.edu

October 2013

CONTENTS

1. INTRODUCTION

The Laser Electron Acceleration Project (LEAP) is a close collaborative effort between members of Professor Byer's group in E. L. Ginzton Laboratory at Stanford University and the Advanced Accelerator Research Department at SLAC National Accelerator Laboratory. The thrust of LEAP is to conduct research on high-gradient dielectric accelerator structures driven with high-repetition rate tabletop infrared lasers. The close collaboration between Stanford and SLAC is critical to the success of this project, by providing a world-unique environment where prototype dielectric accelerator structures can be rapidly fabricated and tested with a relativistic electron beam.

While the promise of large accelerating fields from lasers has already been realized in experiments using plasmas [1,2,3], achieving efficient laser acceleration using a mechanism that is economically scalable to a TeV-class collider has proven more elusive. One promising approach is to make waveguide structures to couple the laser power to the particle beam. While material damage limitations of the waveguide structures will prevent the accelerating gradient from reaching the levels already demonstrated with plasma-based accelerators, there are inherent advantages in using structures that directly couple the laser and the particle beam. Namely, the gains in stability and efficiency, and the scalability to high energies, motivate the further investigation of laser-driven dielectric accelerator structures.

We believe that using lithographic techniques to fabricate dielectric laser-driven accelerator structures will enable their mass production and reduce the cost of future accelerators. Lasers have seen a growth in power and efficiency over the past decade reminiscent of Moore's Law in the semiconductor microchip manufacturing industry. Similar advancements are needed in particle accelerator science and technology if we are to reach the next energy scale in an affordable way. Laser-driven dielectric accelerator structures integrated onto microchips provide a means of reaching this goal.

By leveraging the industry-driven technological advances in lasers and semiconductors, we seek to combine the desirable properties of dielectric materials at IR wavelengths and the mass production capabilities of lithographic device fabrication, to create a compact and cost-effective accelerator structure and laser unit. The challenge, as with RF electron linear accelerators, is to fashion a coupling structure that efficiently extracts energy from the laser source to accelerate charged particles. To this end, we are pursuing three competitive photonic bandgap accelerator structures: 3D photonic crystals (the woodpile structure [4,5,6]), 2D photonic bandgap (PBG) fibers [7,8,9,10], and 1D grating-based phase reset structures [11].

In this report we describe the entire collaborative effort of our group with the AARD group on the laser-electron accelerator project (LEAP) to show the full scope of the work. However, the Budget and the Work Plan are limited to the expenses, equipment, and effort of Professor Byer's group.

A. Particle Accelerator on a Chip

We envision the ultimate form of our dielectric accelerator to be entirely contained on a silicon wafer, which we term an "accelerator on a chip". This envisioned laser-driven particle accelerator will necessarily include: an electron injector, sub-relativistic and relativistic acceleration structures, laser power couplers, steering and focusing elements, and beam position monitors. A conceptual sketch of the accelerator-on-a-chip scheme is illustrated in Fig. 1. Although the illustration depicts a grating-type accelerator structure, we would emphasize that we have developed three competitive accelerator structures in parallel, namely: the 3D woodpile structure, the 2D fiber structure, and the 1D grating structure. Prototypes of each of these three structures have been recently fabricated, as shown in the SEM images of Fig. 2. Moreover, the 3D woodpile structure and the 1D grating structure were fabricated at the Stanford Nanofabrication Facility by graduate students under the prior LEAP grant.

The complete development of all the necessary accelerator elements represents an extensive research effort that extends beyond the immediate research objectives of this proposal. In the upcoming years, we propose to focus our efforts on

i. optimizing the accelerating structure design and fabrication process,
ii. demonstrating an accelerating structure and a beam position monitor,
iii. designing an electron injector, low beta structures, and laser power couplers.

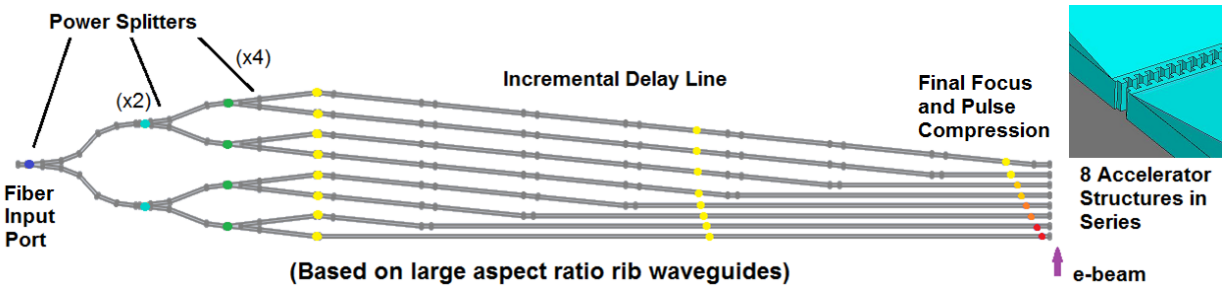

Figure 1: Top view schematic of an envisioned accelerator chip module (approx. 2 cm x 1.5 mm) potentially capable of GV/m gradients. Many such modules can exist on a single wafer, each powered by efficient fiber lasers. The inset shows a 3D view of one of the eight accelerator structures at the end of each waveguide.

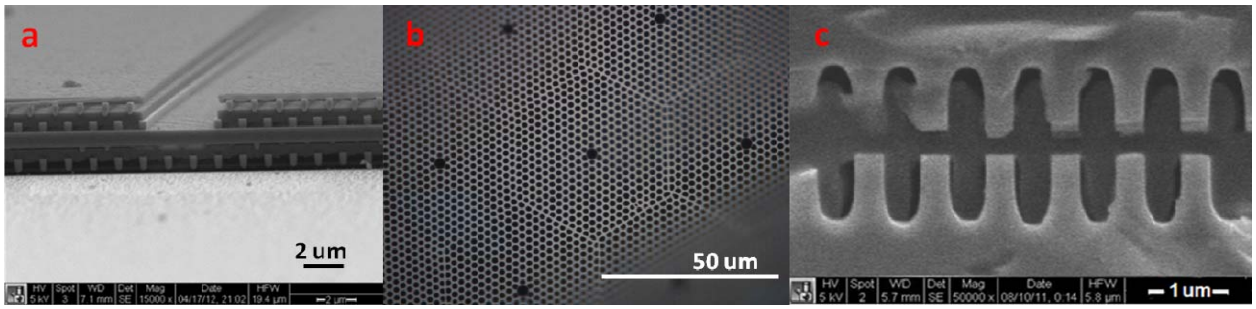

Figure 2: Recently fabricated structures: (a) 3D woodpile, (b) 2D fiber, (c) 1D grating.

2. PROGRESS DURING 2013

A. Summary of progress

The third year of our contract was focused largely on performing beam-based experiments to demonstrate physical principles and the feasibility of dielectric laser-driven accelerator (DLA) structures. To this end, we fabricated two unique optical scale dielectric accelerator structures: the silicon buried grating structure, and the silica grating structure. Both structures were tested in beam-based experiments, demonstrating the successful transmission of a relativistic electron beam through the sub-micron aperture of the structures. Additionally, and most prominently, we performed the first proof-of-principle demonstration of high-gradient laser-driven acceleration in a dielectric microstructure; demonstrating acceleration gradients in excess of 300 MV/m in our silica accelerator structure [1]. Furthermore, we developed and executed a series of beam-based experiments demonstrating the principles of a DLA-class beam position monitor (BPM).

In addition to the beam-based experiments, a significant amount of effort was devoted to preparations necessary to realize the next generation of experiments. We performed extensive measurements to quantify and characterize the laser-damage properties of dielectric materials in order to better optimize our DLA structures. We fabricated grating structures optimized for low-beta acceleration and we constructed an electron beam column specifically fitted for low-beta structure testing. We've begun fabrication on the clam shell BPM structure [3] for high resolution beam position monitoring. We are testing a new fabrication process to simplify the construction of the woodpile accelerator structure. We simulated and optimized efficient couplers for the woodpile structure. And we've begun simulations to understand methods to couple a drive laser to the fiber accelerator structures.

B. Key experimental results from E163

<u>Demonstration of High Gradient Acceleration in a Fused Silica Structure</u>

Since our last report, the improved dual-grating silica structure (designed for 800 nm wavelength operation) has been successfully fabricated and has been tested at the Next Linear Collider Test Accelerator (NLCTA) at SLAC. *In our most recent series of experiments, we demonstrated an accelerating gradient exceeding 300 MV/m [1]. This demonstration represents the first indication of particle acceleration within an enclosed laser-driven dielectric structure operating at optical wavelengths.*

The DLA prototype structure is shown in Fig. 3. Based upon the periodic phase reset structure proposed by Byer and Plettner [2], electrons are accelerated in the gap between two parallel gratings or arrays of etched ridges. Wafers are diced into segments, each containing four micro-accelerators for testing: two with channel gaps of 800 nm and two with 400 nm gaps. The distance between the grating ridges is equal to the wavelength of the laser (800 nm), producing a spatially dependent phase modulation of the laser field that allows correctly phased particles to experience a continuous acceleration.

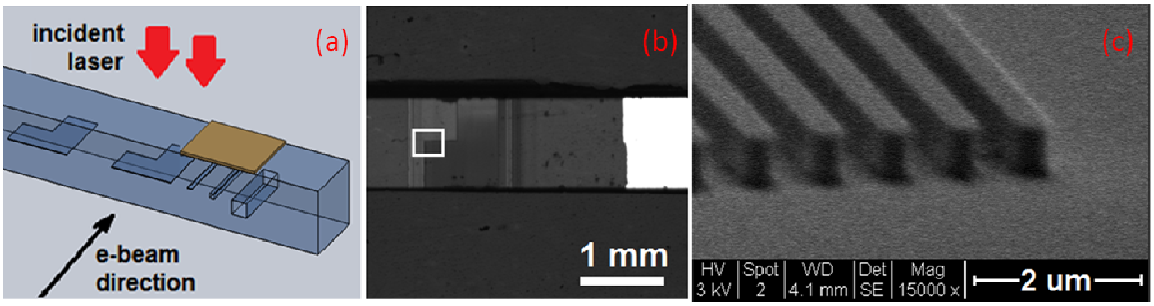

Figure 3: Schematic (a) of the diced test accelerator samples, with (b) microscope image of the sample from above in which the first grating and reflector are visible, and (c) scanning electron microscope close up of the region enclosed by the white rectangle at 15000x showing the boundary of the reduced length 800 nm gap structure.

The energy spectrum of the electrons was measured after they passed through one of the accelerating regions as the laser was alternately turned on and off. Only a small fraction (around 2%) of the electrons in the test beam passes cleanly through the accelerator channel, which has a sub-micron aperture. The particles that hit the dielectric lose significant energy (~400 keV) from collisions in the material and so are easily distinguished from the transmitted particles. There is a clearly visible broadening in energy when the laser is on, due to the fact that particles will either gain or lose energy depending upon whether they pass through the structure at the peak or at the trough of the accelerating wave. The electron beam and the laser beam (both of which are pulsed with 1.5 picosecond pulse lengths) must arrive at the DLA structure simultaneously to produce this interaction. To determine the correct overlap in time, a delay is placed on the laser that varies in a pseudo-random Halton sequence as the data is taken. This is shown in the inset of Fig. 4(a), where the width of the energy spectrum (more precisely, the sigma on the high-energy side of an asymmetric double Lorentzian fitted to the spectra) is plotted as a function of the delay on laser arrival time, and the gradient (extrapolated using the technique outlined in Section C) is plotted as function of laser pulse energy. Given that the interaction length is 0.5mm, the estimated maximum gradient is in excess of 300 MV/m. These values are consistent with the square root dependence on laser fluence, as illustrated by the black curve superimposed in Fig. 4(a). We have also measured the dependence on laser polarization and incidence angle and compared the experimental results with the expected trend from theory and have found agreement in all cases, as shown in Fig. 4(b) and (c).

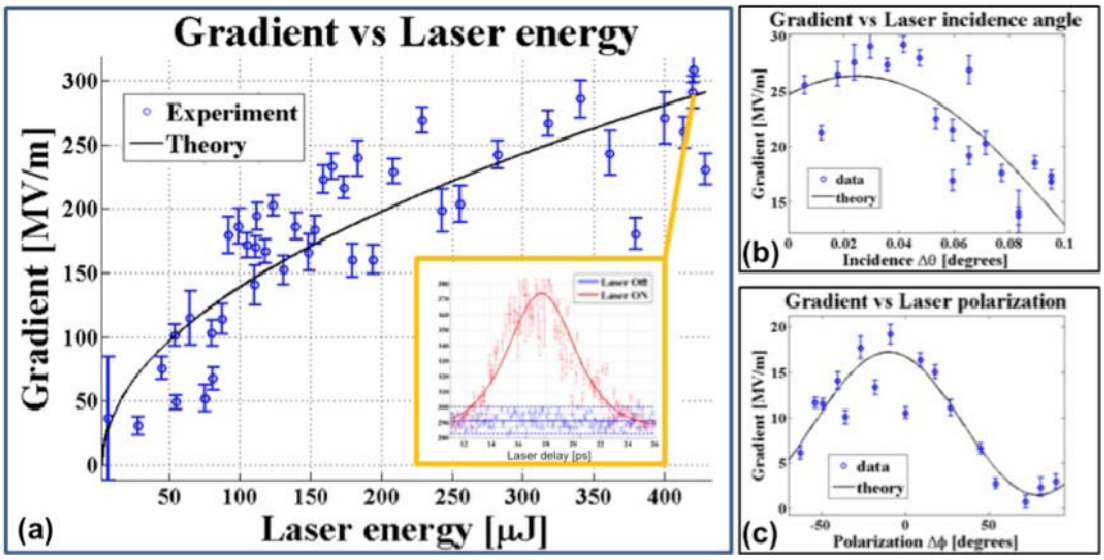

Figure 4: The accelerating gradient of our structure as a function of laser pulse energy (a), laser incidence angle (b), and laser polarization (c). Each data point represents a cross-correlation of the laser pulse and electron bunch (inset).

Observation and Measurement of Wakefield Radiation in a DLA Device

We have begun our efforts to demonstrate a grating-based beam position monitor (BPM) [3]. Our first efforts focused on demonstrating the principles of operation of the grating BPM by verifying a strong dependence of the radiated electron beam wakefield as a function of the BPM structure geometry. The experimental setup for this experiment closely mimics that of the grating acceleration experiment, except that in this experiment we are transporting an electron beam through an unpowered grating structure and monitoring the beam-generated wakefield radiation. For the initial set of experiments, we used the grating accelerator structure as our BPM structure.

The results of our initial experiments verified many of the physical principles expected from our BPM structure. The wakefield radiation generated by the electron beam was easily detected by a room temperature PMT, even when coupled through an optical spectrograph. We find that the radiated wakefield from our grating structure has a single peak at 782 ± 3 nm, which closely matches the periodicity of the grating structure (800 nm). Furthermore, we find that the radiated wakefield is linearly polarized, with the electric field parallel to the electron beam trajectory and perpendicular to the grating teeth, as expected. These results are shown in Fig. 5. Both of these results strongly agree with theory and reject the possibility of optical transition radiation or Cherenkov radiation as the primary radiation mechanism. In the coming year, we will continue advancing the grating BPM experiments by fabricating custom grating structures with a series of discrete grating periods. We will then test these discrete BPM structures to verify a position-dependent radiation wavelength.

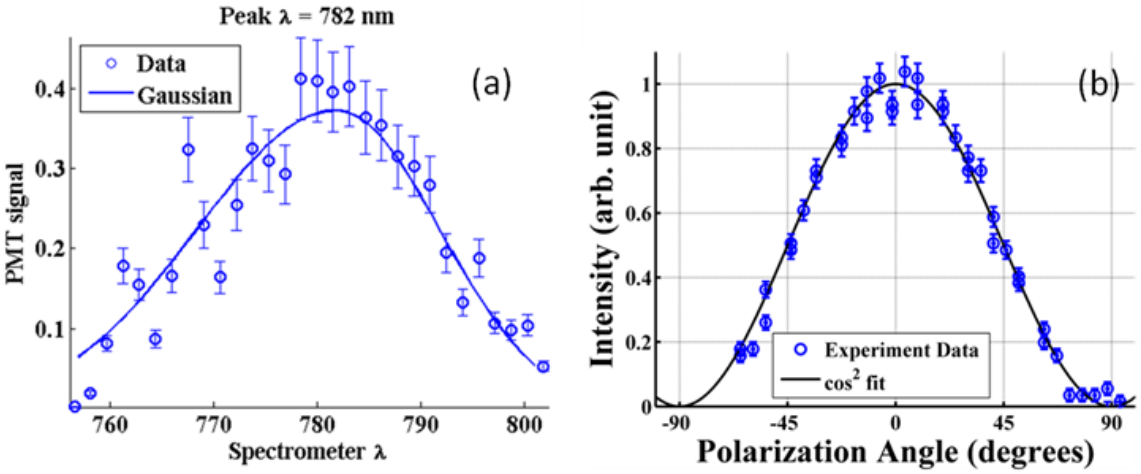

Figure 5: (a) Wavelength signature of the ebeam wakefield signal. (b) Wakefield signal as a function of polarization with respect to the gratings.

First Beam Tests of a Silicon Buried Grating Structure

We reported above successful first demonstrations of high gradient (300 MV/m) acceleration in a fused silica dielectric accelerator driven at 800nm wavelength by a Ti:Sapphire laser system. We have been developing an optimized accelerator structure based upon similar operating principles, but constructed from silicon using a monolithic design powered at 2 μm wavelength. This alternative design provides several potential benefits, including improved efficiency and alignment, relative ease of fabrication and integration of components, and compatibility with Thulium based solid state fiber lasers, which we plan to use in future to demonstrate high repetition rate operation of these devices. Initial fabrication efforts on this structure were reported in prior quarters. The fabrication process has since been modified to include a number of new features that are illustrated in Fig. 6. The figure shows a SEM scan of the front face of the structure with the electron beam direction out of the page.

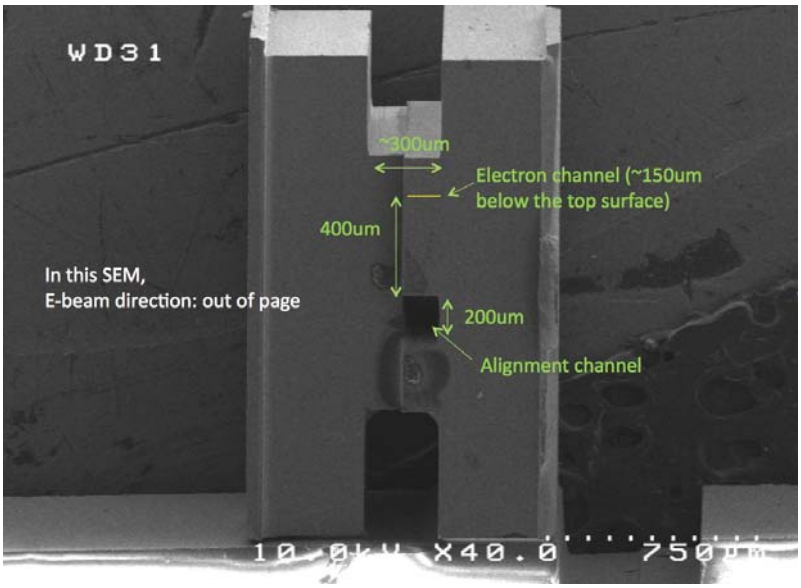

Figure 6: First beam test prototype of silicon buried grating structure.

The electron accelerating channel is a 1-micron tall etched groove (highlighted by a horizontal yellow line in Fig. 6) approximately 50 microns wide and lying 150 microns below the surface of the material at the bottom of a 300 micron wide trench. The accelerator is powered by illuminating the accelerating channel with a 2-μm wavelength laser pulse incident from above (top to bottom in Fig. 6). For power demonstration and electron beam tests, 2 μm laser light will be provided by an available optical parametric amplifier (OPA) with a wavelength range of 1 to 2.5 μm. To provide the needed 50 μJ pulses from the OPA, a new Coherent regenerative amplifier with 5 mJ pulse energy operating in picosecond mode has been commissioned at the SLAC NLCTA facility to use as a seed laser for this system. A new transport line for 2 μm light has been installed to deliver the laser to the experiment.

The buried grating prototype structure was subjected to electron beam tests at the SLAC NLCTA facility to demonstrate transmission of the particle beam through the narrow (2 micron) gap of the accelerating channel. It should be noted that although the 5pC electron beam is tightly focused, the typical spot sizes of 10 to 20 μm RMS are still significantly larger than the vacuum aperture of the accelerating channel. Consequently, even with an optimally positioned and angularly aligned sample, only about 1% of the particles (roughly 50 fC) transmit cleanly through the aperture, while the bulk of the particles strike the material and lose energy due to collisional losses. Consequently, if a comparable 1-2% fraction of beam particles escape over the top or sides of the sample the resultant degradation in signal-to-noise ratio will impede verification of the transmitted component. The vertical separation distance of 150 μm shown in Fig. 6 between the channel and the top edge of the structure was therefore chosen carefully in this design iteration to mitigate any leakage of particles over the top edge while minimizing laser propagation distance in the material for future studies using a vertically incident laser beam. In the electron beam transmission tests from the present quarter, the transmitted population was clearly observed for the first time on 1 of 3 identical samples that were mounted together on a single substrate and selectively moved into the electron path one at

a time. Transmission was observed on the other two samples as well, but it was comparatively weaker. The discrepancy is believed due to angular errors in the technique for mounting the samples. At present the samples are mounted by adhering them to a fused silica substrate with epoxy applied at the edges. An etched trench in the substrate material alongside the sample (seen on the bottom right of Fig. 6) provides a fiducial, but the alignment is not directly registered to this feature. In addition, the bottom edge of the sample is cut by wafer saw, which can produce uneven edges and protruding features. In conclusion, the device fabrication and design appear suitable for future acceleration tests, but alternate mounting techniques will be explored in the next quarter in order to improve angular alignment of the mounted samples. In the coming year, we will perform first experiments with laser illumination of the structure using the new system.

C. Theoretical and numerical modeling

Analytical Model for Gradient Extrapolation in the Dual Grating Accelerator

In order to fully understand the experimental results of the high-gradient demonstration reported in Section B, we have developed an analytical description and model of the laser-electron interaction for the case of a long electron bunch (much longer than an optical cycle). In our model, we partition the long electron bunch into a series of short finite slices (much shorter than an optical cycle) and calculate the effects of the laser on each of these slices, as shown in Fig. 7a. Since these slices are much shorter than an optical cycle, they will experience a net change in energy (gain or loss), with negligible effect on their initial energy distribution, see Fig. 7b. The net effect of the laser on the long electron bunch is then the summation of the effects on each slice. We find that the predicted effect on the electron energy distribution is a division of the energy spectrum from a single peaked profile to a double peaked profile, shown in Fig. 7c. We find a strong agreement when comparing the analytical results to the actual effects observed in the experimental data, and therefore use the analytical model to interpret an accelerating gradient from the experimental data.

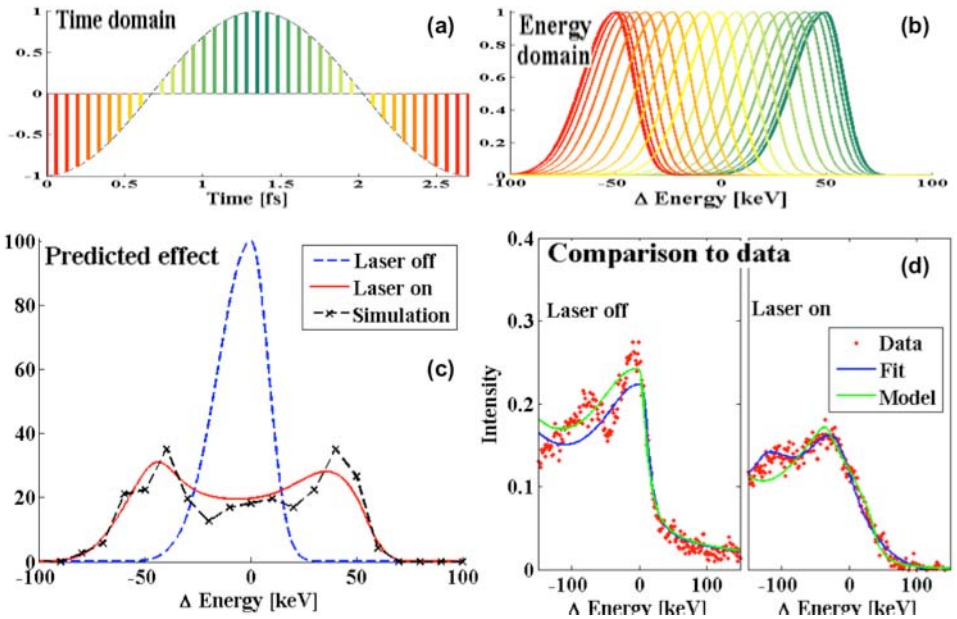

Figure 7: Analytical model of the laser-electron interaction in the time (a) and energy (b) domain. The predicted effect of the laser modulation on the electron energy profile (c) and the comparison to experimental data (d).

High-efficiency Power Coupling in the Woodpile Structure

For the 3-D PBG accelerator case, silicon guides may be naturally integrated to the silicon woodpile structure by photolithography. However, much like the conventional RF cavity-disk loaded (RFQ) accelerator structure, a woodpile defect waveguide exhibits longitudinal periodicity. Because of this translational variant nature, a cross-sectional matched incident mode profile will be insufficient to launch the propagating mode in the woodpile waveguide properly, resulting in signifficant standing waves. Standing waves would tighten tolerance to fabrication errors and make the structure susceptible to high power breakdown. A travelling-wave launch method based on scattering matrices has previously been developed for RFQ accelerator structures (Nantista et al., 2004), and could be applied to the woodpile waveguide. A mode launcher made of a two-dimensional waveguide, such as a silicon guide in the woodpile accelerator case, with a perturbation to form a coupling iris, can excite all the space harmonics needed to compose the propagating mode. A one-quarter cutaway cross-section of such a scenario is illustrated in Fig. 8. This figure shows transverse coupling from a silicon light guide of TE operation to a TM mode accelerating channel in the woodpile structure. An embedded piece of perfect conductor, or other material, inside the silicon guide (red rectangle on the left of Fig. 8) serves as a coupling iris to optimize the traveling wave match to the TE guide, which has been optimized in simulation to better than 95% coupling efficiency.

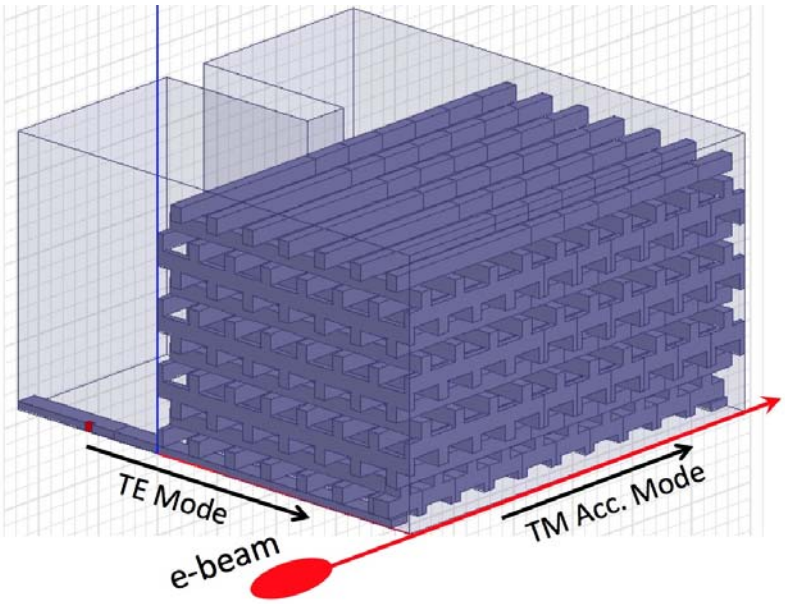

Figure 8: HFSS simulation geometry for high-efficiency transverse power coupling to the woodpile structure from a TE mode silicon guide to a TM-like mode accelerating channel where the electron beam (red ellipse) would travel.

Standing Rod Accelerator Structure

We have also investigated a new silica rod array structure for laser driven acceleration. The structure consists of two rows of circular or elliptical dielectric rods equally spaced on a substrate, as shown in Fig. 9 (left). The electrons travel between the rows of material. One of the advantages of this structure is that all the rods are fabricated on a single substrate, therefore positioned and aligned with photolithographic level precision. Similar to the dual-layer rectangular grating structure, the periodic arrangement of the rods along the beam channel provides the necessary phase reset of the electromagnetic fields and therefore required phase synchronicity for laser acceleration of the particles. Fig. 9 (right) plots the simulated longitudinal E-field in the accelerating gap when the structure is illuminated by a plane-wave. Although notable gradients are predicted with circular rods, the acceleration factor (ratio of peak fields in the channel vs peak fields in material) can be optimized with elliptical shaped rods. Acceleration factor as high as 0.45 can be realized with an ellipse aspect ratio of 0.767.

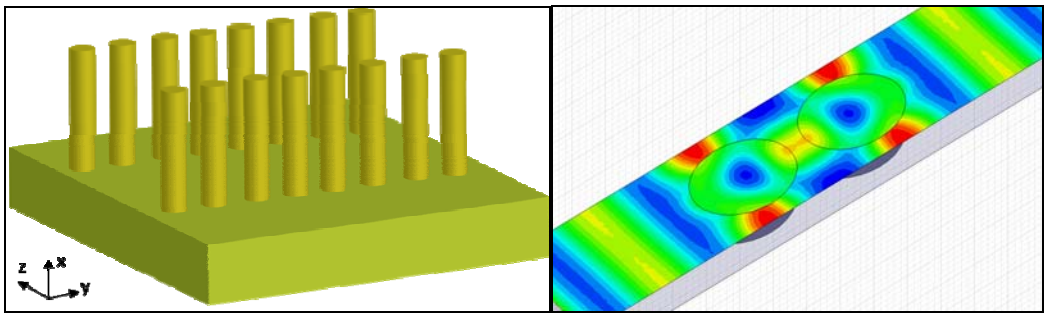

Figure 9: (Left) Layout of the dielectric rod array accelerator structure. (Right) Simulated longitudinal E-field profile of one period of the structure, with a plane-wave excitation.

Simulations of Coupling in Hollow-Core Fibers

An efficient coupling method has also been developed for a hollow-core dielectric structure based on the cylindrical Bragg arrangement [4]. The structure consists of a central vacuum channel surrounded by alternating layers of dielectric material forming a narrow-band reflector. These alternating layers have different dielectric coefficients and act as a Bragg mirror that confines the electromagnetic fields to the vacuum channel. The individual thicknesses of these layers were specifically designed to support a traveling-wave accelerating mode in the vacuum channel. Compared with the woodpile structure, mode confinement uses a 1D rather than 3D photonic crystal. However, the cylindrically symmetric geometry helps ensure single-mode excitation and a pure TM_{01} mode with uniform field across the beam aperture. Laser power is coupled into and out of the structure via two input and output arms of dielectric material, as shown in Fig. 10, which displays a wedge-shaped section of the structure from a simulation using the commercial finite element frequency domain electromagnetics code Ansoft HFSS. Coupling efficiency is calculated by evaluating the power transmission coefficient between the waveports (labelled "port 1" and "port 2") on the faces of the input/output guides.

The best performing structure to date has achieved a transmission coefficient of 88% from the input (port 1) to the output arm (port 2) and successfully couples the accelerating mode into the accelerating guide vacuum channel of the structure, as shown in Fig. 10. The efficiency of the structure is sensitive to the length of the acceleration region and the shape of the region where the input arm and the vacuum channel meet. There are perfect electric boundaries on the outer radius of the structure and absorbing boundaries at the edges of the unit cell currently being tested in simulation. Further optimizations of the design will seek to improve the efficiency of the coupling and the quality of the accelerating mode produced. The conducting boundaries, which are a computational expedient, will be removed in favor index guiding of the laser power and open outer boundaries, since metal surfaces are ultimately undesirable from the standpoint of laser damage and power loss. Fabrication techniques for this acceleration structure are currently being investigated.

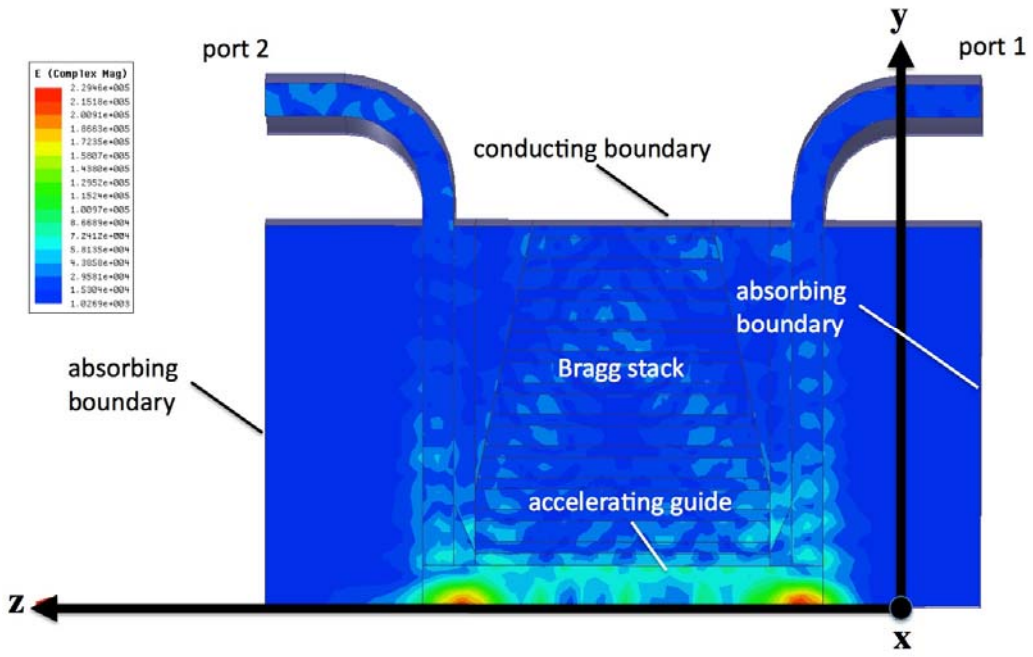

Figure 10: HFSS simulation of complex electric field magnitude, showing successful coupling of input power from the arm on the upper right into a traveling wave TM_{01} like central waveguide mode along the z-axis.

Wakefield Simulation in PBG Fiber Accelerators

We previously reported successful experimental observation and spectral analysis of radiated wakefields in a commercial hollow-core optical fiber with an operating band centered at 1060 nm wavelength. The commercial HC1060 fiber was carefully modeled based upon scanning electron micrograph (SEM) images taken at Stanford University. Fig. 11 shows a recent SEM image of a HC1060 sample with a = 2.13 μm, that was used in the wakefield experiments. The core of the fiber is a circular region, which is the PBG lattice, surrounded by a cladding with a thickness about the diameter of the lattice region. The lattice has a central defect whose size is much bigger than the other lattice holes when compared with the Lin fiber in the previous section. The lattice holes are separated by dielectric vertices and webs whose dimensions are on the order of sub-microns. Simulation using BandSolve shows that the web thickness determines the bandgap location with thicker web making lower bandgap frequency. The glass vertices determine the bandgap width, with more glass making wider bandgap. More detailed SEM measurements will be carried out to elucidate more accurately the vertices and web dimensions. For T3P simulation, the lattice period a = 2.75 μm, the defect diameter 9.6 μm, the vertex size $b = 0.16a$, and the web thickness $t = 0.036a$ have been used.

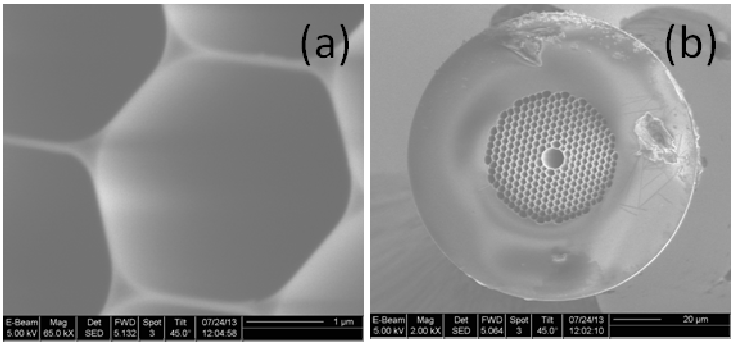

Figure 11: (a) SEM image of a sample HC1060 commercial fiber; (b) Close-up image showing the glass webs and vertices connecting the vacuum hexagonal-shape holes.

The T3P simulation of the HC1060 fiber assumes a perfect symmetry of the lattice, so that a 30^{o} slice is sufficient to model the full geometry for the excitation of an axial beam. A Gaussian bunch of RMS σ = 0.3 μm enters from the left boundary and transits through the fiber with a length of 20*a*. The frequency content of the Gaussian bunch covers the bandgap frequency range as well as that contributed by mostly the cladding modes located near the edge of the fiber. Fig. 12 shows a snapshot of the wakefield generated by the transiting beam. The trailing field inside the lattice indicates possible excitation of the fiber modes and the field in the cladding demonstrates Cerenkov radiation because of its higher dielectric constant. The simulated model has a shorter cladding width than that shown in the SEM image. This will mostly affect the excitation of the cladding modes and the effect on the lattice modes is small. The radiation field is monitored as a function of time outside the HC1060 structure, from which the mode spectrum is obtained by the Fourier transform of the radiated signal.

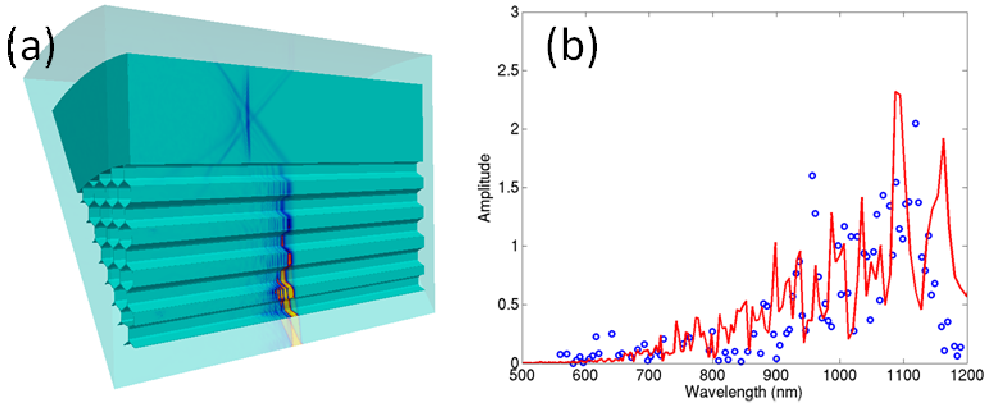

Figure 12: (a) Snapshot of T3P simulation of beam transit through the HC1060 fiber enclosed in a vacuum region. The beam enters the structure from the left end and exits at the right; and (b) comparison of simulation (red) and measurements (blue) for the radiation spectrum generated by a beam transit in the HC1060 fiber.

Fig. 12(b) shows the comparison of the radiated spectrum obtained by simulation and measurements. The spectrograph measurement in the experimental setup ranges from 550 nm to 1200 nm with 3 mm resolution step, which is comparable to the resolution of the time domain simulation. It can be seen that the simulated spectrum is in good qualitative agreement with measurements. It should be pointed out that modes of lower frequencies (or longer wavelengths) are also found in simulation. They are likely the modes generated in the cladding region of the HC1060 and will radiate away at short distances. The spectrograph measurement can be extended to the lower frequency region to determine whether the cladding modes still contribute to the signal measured at large distance from the beam excitation region.

D. Structure fabrication and benchtop testing

Grating Accelerator Fabrication

The previously reported process to fabricate the grating accelerator structures has been modified to achieve improved alignment during the overlay and bonding steps, as well as improved uniformity across the bottom and top gratings of the structure.

A schematic of the new process is shown in the Fig. 13.

To improve the overlay alignment, there is now a step 0 which consists of patterning global alignment marks via metal evaporation of Chromium on the fused silica substrate. Additionally, the process is now symmetrical, so both top and bottom wafers are processed identically, removing unwanted variations in structure geometry. The main process steps remain the same, etching a trench that defines the structure gap (step 1), etching the gratings inside that trench (step 2), and then bonding (step 3) and dicing (step 4) two such wafers.

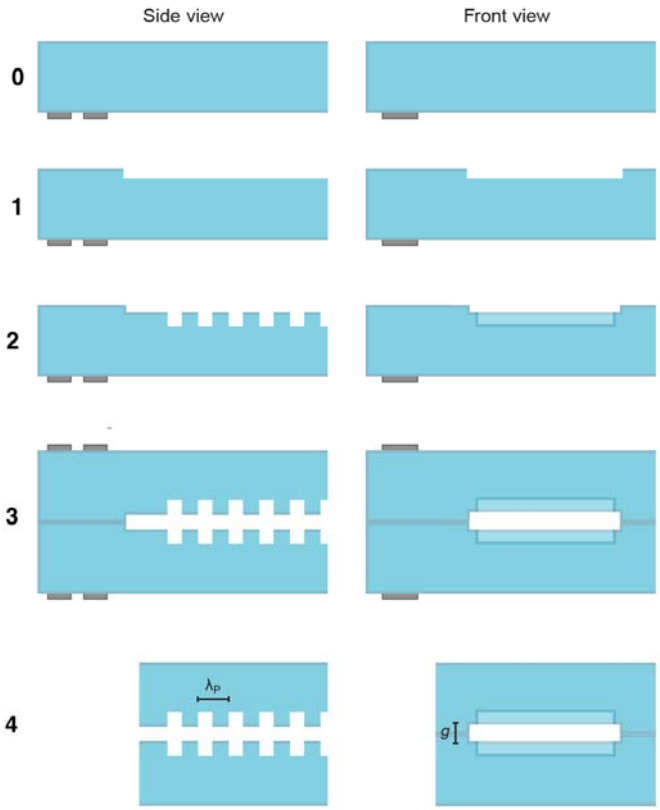

Figure 13: Grating structure fabrication process.

To improve alignment during bonding (step 3) we designed a new set of alignment marks made up of gratings as shown in Fig. 14.

When etched onto the fused silica substrate during the same exposure that defines the accelerator's gratings (step 2) these marks provide a high contrast feature that is easy to find and align under the microscopes of an Electronic Vision ALIGN tool. With the marks of the top and bottom wafers properly aligned (dark crosses inside clear crosses) the alignment is better than 3 microns.

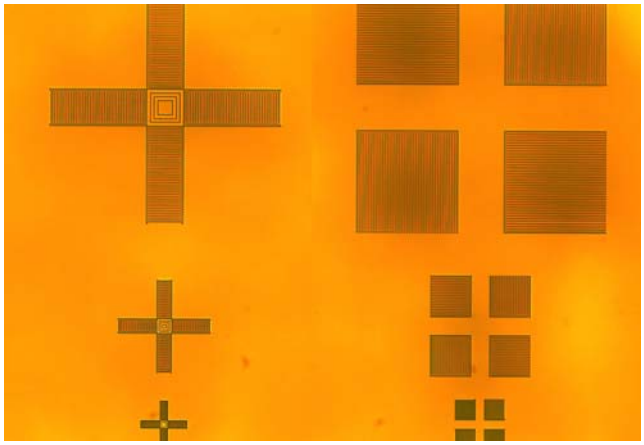

Figure 14: Alignment features on silica substrate.

Beam Position Monitor Fabrication

To demonstrate the basic principle of operation of the clamshell grating BPM structure we've fabricated a discrete BPM structure to simplify the experiment. The structure contains only four different grating periods: 1000, 1130, 1260, and 1390nm, each 250 microns wide, chosen so that they generate a clearly distinct wakefield radiation peak wavelength as the electron beam is shifted transversely across the structure.

The fabrication process is identical to that described in the previous section, except that the pattern of the gratings in step 2 is now that corresponding to the BPM structure and not the accelerating structure. A microscope image of a finished BPM structure is shown in Fig. 15. The lighter regions which form a square delineate the boundary of the 800 nm wide trench. Inside this trench is a 1mm x 1mm box where the four gratings of different period can be observed.

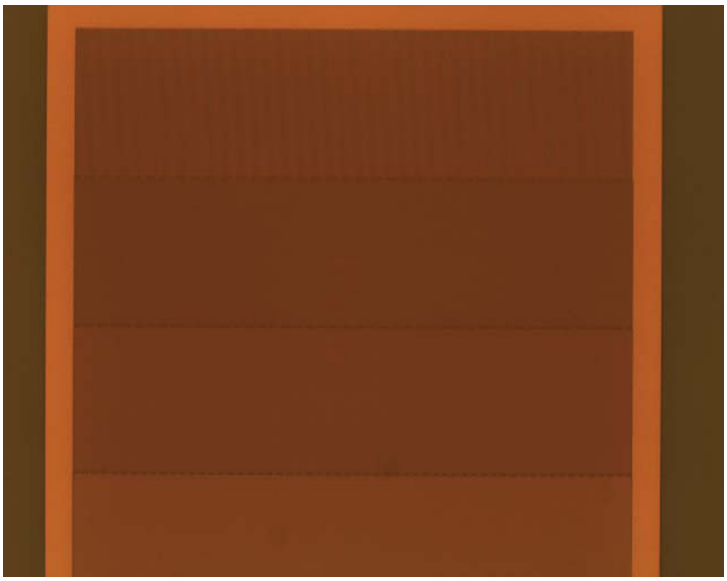

Figure 15: Discrete periods on the BPM structure.

Low Beta Grating Accelerator Structure Fabrication

We have previously reported successful demonstrations of electron acceleration in DLA structures operating at both relativistic and non-relativistic energies. Optimized structures are needed that operate in both of these regimes in order to successfully accelerate particles directly from an emitter source up to relativistic (speed-of-light) energy in a short distance. To these ends, a modified prototype of the fused silica dual-grating accelerator has been fabricated for sub-relativistic electron acceleration from a 30 keV electron source. In order to account for the dephasing length and electron charging effects that become relevant at sub-relativistic particle energies, the new bonded dual-grating design consists of elevated grating surfaces etched onto a "mesa" 34 microns in length along the intended electron path and embedded within a larger (1mm long) diced substrate. The modified fabrication process is described in Fig. 16 (step 0 not shown).

Steps 1 and 2 are the usual grating-defining steps, although in this particular case we target 200nm gap structures, so the initial trench (step 1) is only 100 nm deep. The gratings have a period of 750 nm (the corresponding 3rd harmonic for a nominal 28keV beam at MPQ) as defined via optical lithography. An SEM image of the gratings is shown below (A). Work is under way to pattern 250 nm period gratings using e-beam lithography in order to utilize the first field harmonic.

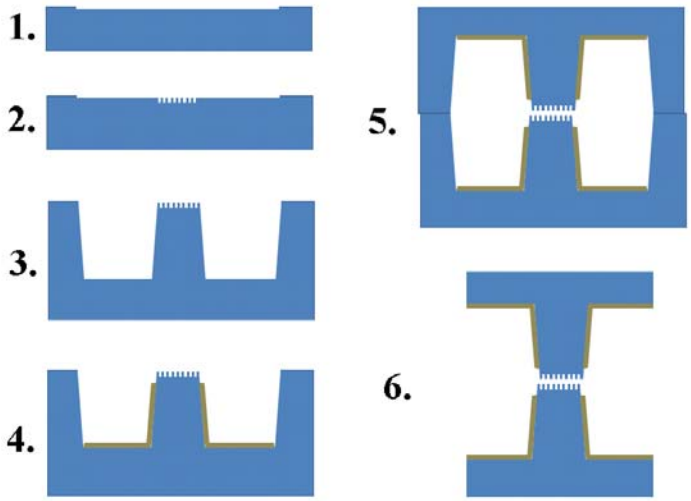

Figure 16: Low-beta grating structure.

The Rayleigh range of the relativistic beams that can be used to test this structure is in the order of 50 um, so the beam quickly diverges outside the 34um grating region. Removing material outside this region by defining the mesa as shown in step 3 helps minimize the unwanted charging effects from the enlarged beam traveling in close proximity to the structure walls. Fig. 17 shows the 34 um wide photoresist mask used to perform this etch, covering the grating region.

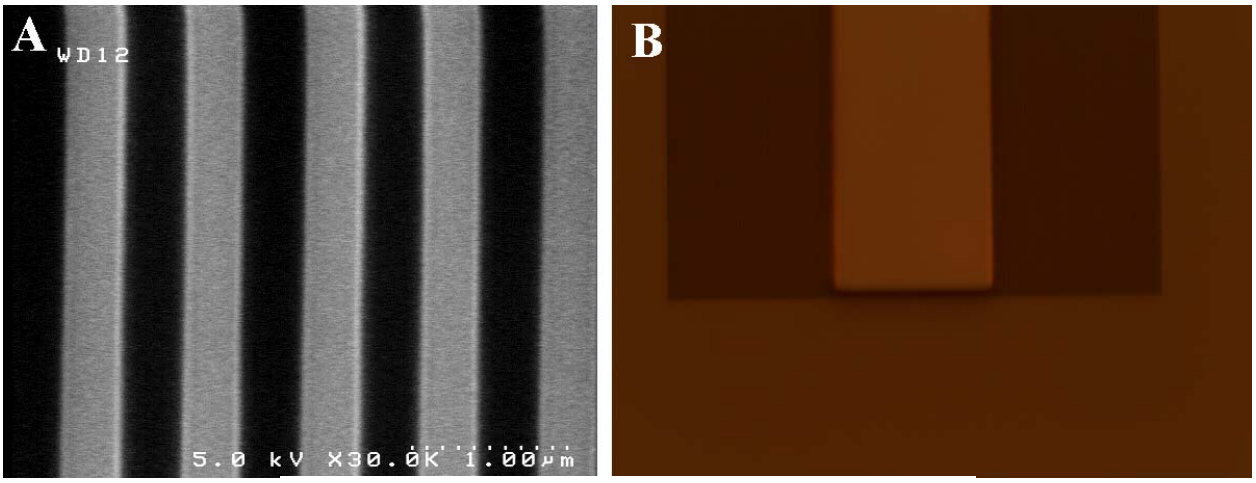

Figure 17: SEM images of low-beta grating structure.

Silicon Buried Grating Structure Fabrication

We completed our fabrication process of prototype silicon buried grating accelerator structures. The fabrication processes and results are illustrated in Fig. 18. Starting with silicon wafers with a layer of thermal oxide for the hard mask, we transferred the accelerator patterns from the photoresist to the oxide layer, followed a 50µm deep etch using deep reactive ion etch (DRIE). After depositing low temperature oxide to protect the accelerator structure, we used another set of optical lithography and etching steps to create a large, smooth surface for laser illumination. This was followed by hydrogen annealing of the wafers to smooth out the scalloping of the sidewalls from the DRIE process. Finally, we grew a 190 nm layer of thermal oxide to further increase the accelerating gradient, as predicted by our design and simulation. We diced the wafers and accelerator dies were fixed to blank dies to make an assembly suitable for optical beam and electron beam testing. In the next quarter, we plan to start laser driven-beam testing of our buried gratings, including the design and implementation of the optical setup at SLAC for 2 µm laser illumination. A schematic of the beam experiment is shown in Fig. 19.

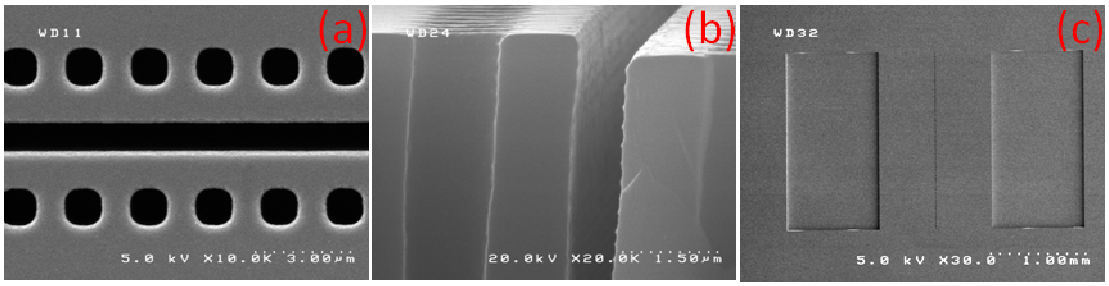

Figure 18: SEM images of the buried grating accelerators after hydrogen annealing at 1100C for 5 minutes, (a) top view, (b) cross-sectional view, and (c) top view of the whole device

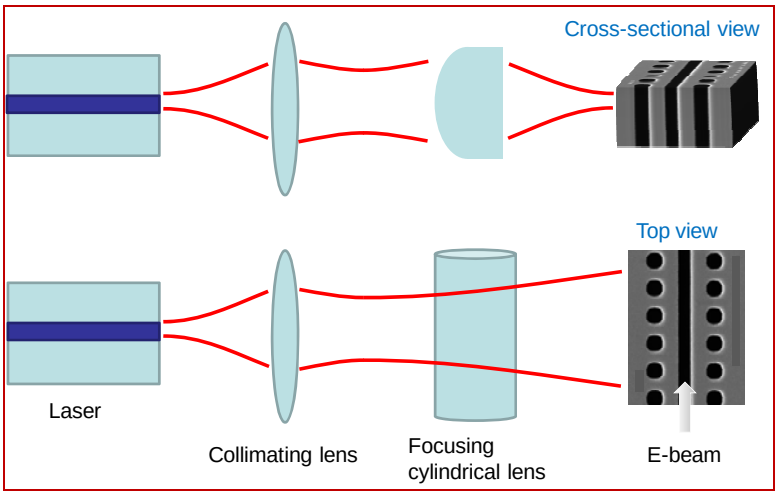

Figure 19: Schematics of the optical setup for buried grating accelerator testing at 2 μm

Fabrication of the Standing Rod Structure

The procedure for creating the silica rod array structure is to first fabricate the rods in silicon and then oxidize the rods to form silicon dioxide. This takes advantage of the available deep etch chemistry for silicon while capitalizing on the high laser-damage resilience of silicon dioxide rods. In this method, a 600 nm thick negative tone resist, Hydrogen SilsesQuioxane (HSQ), was spun on a silicon wafer and subsequently exposed by an electron-beam lithography tool at 100 kV energy. After development the pattern was transferred to silicon in a high-density plasma etching tool using chlorine chemistry. The etched depth was about 10 micrometers. The conversion into silica rods was achieved through wet oxidation at around 900 degrees Celsius. Preliminary fabrication of a circular shaped rod array has been done, with SEM images of a prototype structure shown in Fig. 20. From Fig. 20(b), we find that the circular shapes are well defined, and the center-to-center spacing of the rods is roughly the desired 3 um period. From the side view in Fig. 20(a) we find that the rods have uniform height of 10 um.

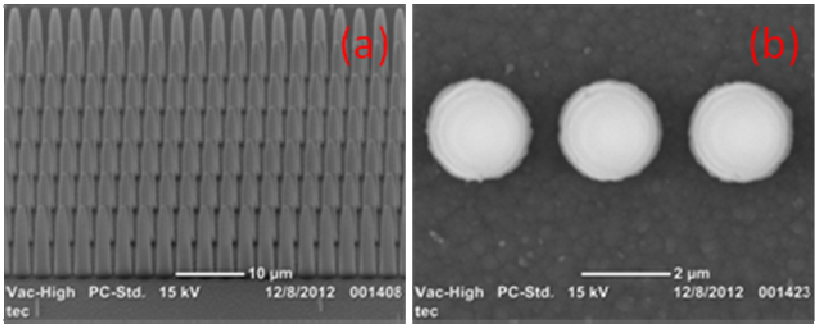

Figure 20: Side-view and top-view SEM images of a fabricated silica rod array structure.

Fabrication of an 18-layer woodpile structure

Previous efforts to fabricate a silicon woodpile accelerating waveguide used a layer-by-layer photolithographic process [5] or a combination of direct laser writing and silicon double inversion [6]. However, the layer-by-layer process suffered from stress accumulation and the double inversion process produced elliptical (rather than the optimal rectangular) features. A new approach to form 3D woodpile structures is being pursued, based on stacking pre-fabricated woodpile layers. This technique does not require high temperature processes and is flexible on material choice. Additionally, this approach allows for enough mechanical robustness to assemble a complete waveguide structure(as opposed to post-assembling two halves of the hollow waveguides [5]). The fabrication process is faster, simpler and more cost effective than previous 3D photonic crystal manufacture methods, making it ideal for the fabrication of a variety of optical, chemical, and electronic devices.

The overall fabrication process is depicted in Fig. 22. The woodpile pattern is first etched into the top layer of an SOI wafer, and then released from the substrate with HF wet etch. The released membrane is consequently transferred on top of a PMMA film, separated from a Si substrate by a PVA film (PRs films). Then the woodpile membrane on PMMA/PVA (PRs) is again mounted on a handling Si wafer with an opening at the center where the woodpile structure will be located. This handling wafer will be flipped with the PRs/woodpile facing down and then aligned and stacked onto an unpatterned substrate or over previously transferred woodpile layers. After dissolving PRs in acetone and water, more woodpile layers can be stacked on.

The 18-layer woodpile structure in Fig. 21 differs from the desired structure in that the alignment between the layers are not accurate. However, this proof-of-concept shows that it is possible to transfer and stack Si membranes to fabricate woodpile structures.

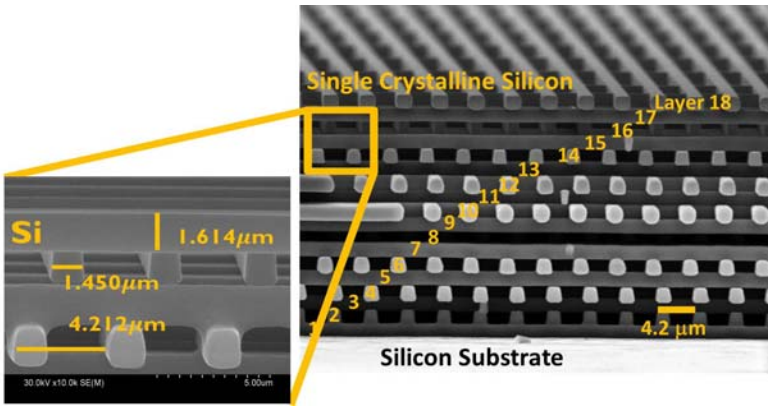

Figure 21: The woodpile structure with critical lattice parameters marked, W = 1.2 μm, Δa = 4.2 μm and h = 1.6 μm, respectively.

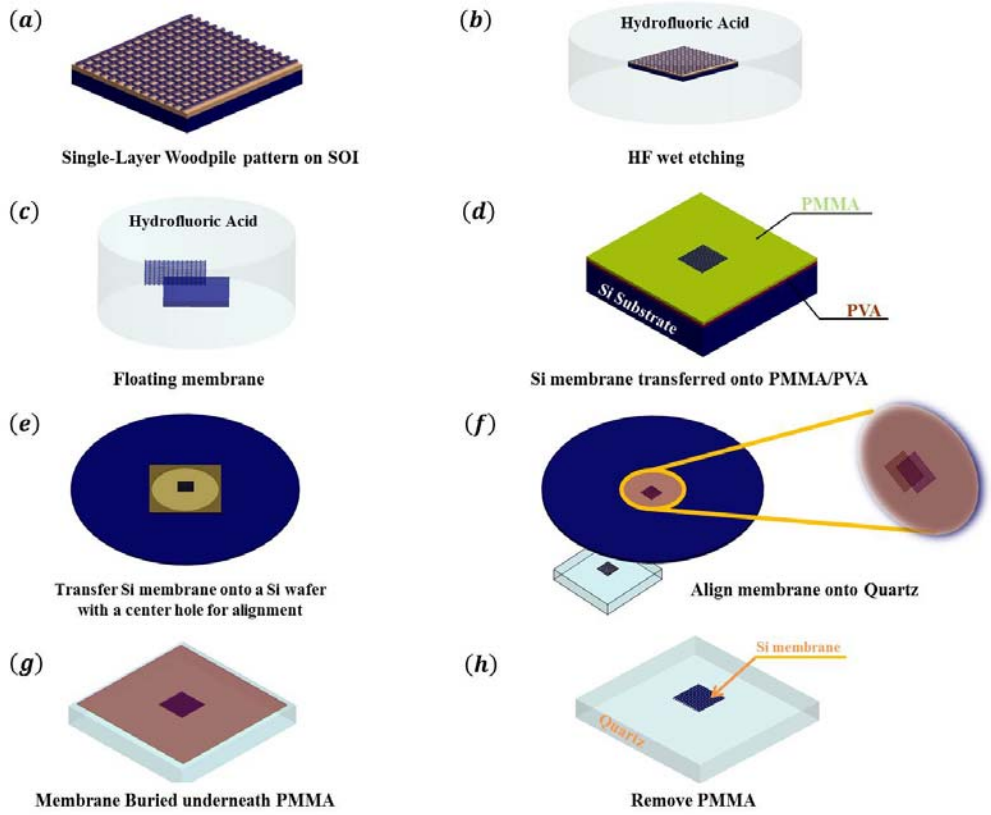

Figure 22: Schematic of the silicon membrane transfer process.

Our recent efforts on this front focused on attaining accurate alignment between layers. We identify the following features as necessary for an alignment and bonding system: precision stages to control both the lateral position of the wafers and the gap between the wafers; a system to ensure good wafer parallelism; a monitoring method to determine the relative positions of the two wafers; and an effective procedure to ensure good alignment during the wafer-contact process. Figure 23(a) shows schematically the new system that we have developed. In order to improve the degree of control in the lateral direction, we use a 5-axis Pico-motors with high resolution and high linearity, along with an Olympus SZX9 stereo microscope capable of 9.5X to 85.5X magnification .As shown in figure 23(c), we achieved alignment within 300 nm using this setup. We believe that we can further reduce the overlay error to 60 nm.

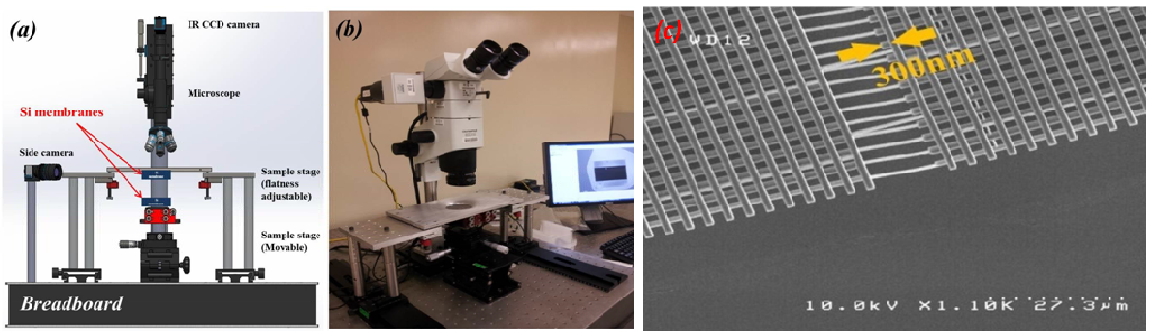

Figure 23: (a) Schematic of the new high-precision alignment/bonding system. (b) The alignment system at installed at Stanford. (c) Demonstration of 300 nm overlay error with new alignment stage.

Development of an In-Vacuum Test Stand for Damage Testing

As we evaluate accelerator designs with integrated optics, the laser damage thresholds of the subcomponents will also be tested for maximum power delivery capability. These structures may include Al_2O_3 and Si_3N_4 wide aspect ratio waveguides, SiO_2 based waveguides, as well as various splitting and coupling devices for the integrated waveguide network. In the past year, the newly constructed in-vacuum laser damage setup, shown in Fig. 24, was fully commissioned and first laser damage testing of patterned substrates initiated at 800nm wavelength. In addition, the optical parametric amplifier (OPA) was moved adjacent to this test stand. This will allow both for damage testing of materials, and for laser powered tests of the prototype relativistic electron accelerator devices at wavelengths from 0.8 to 2 microns.

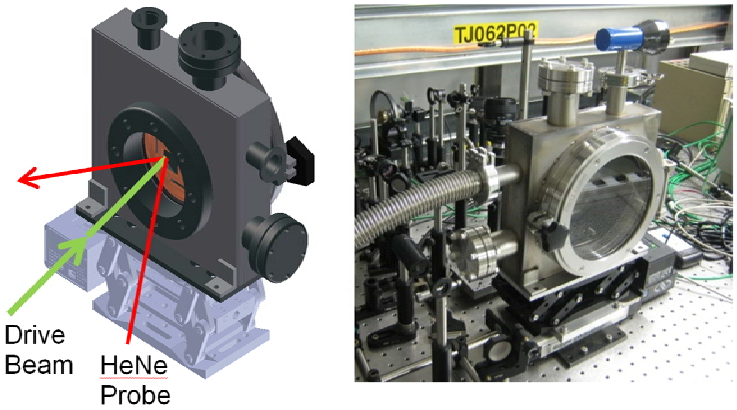

Figure 24: High vacuum laser damage threshold test setup schematic and image.

The new in-vacuum damage threshold test station was commissioned and the first in-vacuum damage threshold measurements were conducted on patterned DLA structures from the same wafer as the one used in the successful acceleration experiment reported last quarter. An array of accelerator structures was placed in the vacuum chamber at a pressure of 10^{-5} torr. The IR pulses from our Ti:Sapph laser system were then focused to a RMS spot size of 27 x 53 μm^2 and incident on the structure, in the same manner as in

the acceleration experiment. The laser fluence was then gradually increased from an initial value of 2.00 μJ in increments of 1.85 μJ, while the illuminated site was monitored with a camera. At each energy level approximately 5000 laser pulses were impinged on the structure. Damage was determined to occur when a visible change in the strength and consistency of the scatted IR light at the illumination site was observed. A total of 24 independent damage threshold measurements were taken and each damage site was afterwards inspected under a high powered optical microscope to verify the occurrence of laser damage (see Fig. 25).

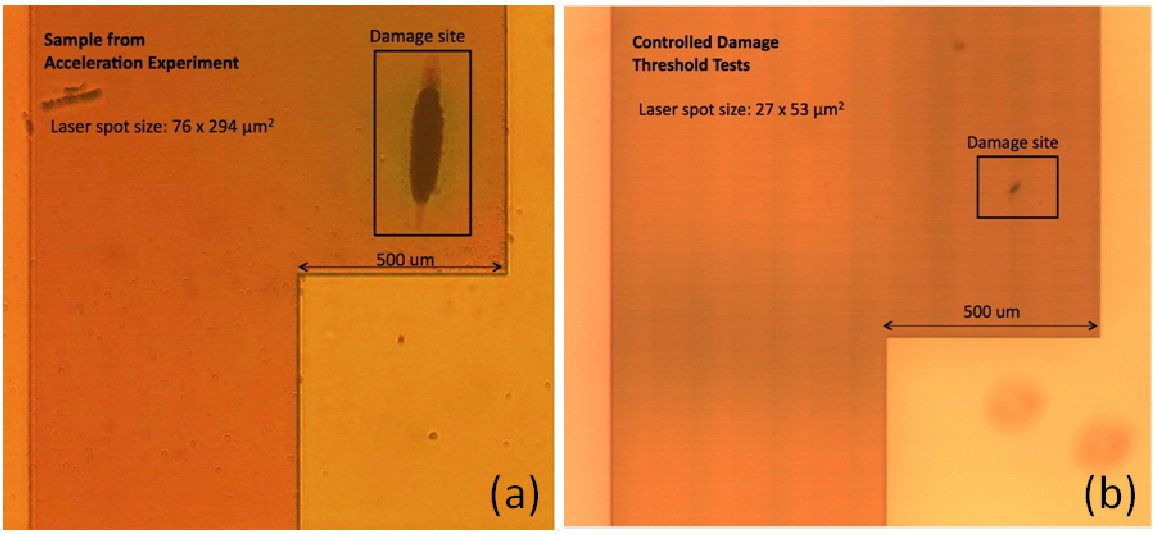

Figure 25: Optical microscope images showing damage sites from (a) the sample used in the acceleration demonstration experiment and (b) a controlled measurement of in-vacuum laser damage threshold on a similar structure not exposed to the electron beam.

The results of these measurements indicate a laser damage threshold of 0.85 ± 0.14 J/cm^2 for our grating accelerator structures. From post-examination of the structure it is clear that this damage threshold value was exceeded during the course of the experiment, as seen in Fig. 25(a). However, we continued to see acceleration up to the maximum available pulse energy. Based on post analysis of a laser damage site, we deduced that our laser RMS spot size during the experiment was 76 x 294 μm^2, yielding a maximum fluence of 0.85 J/cm^2 on the gratings. In the coming quarter, these studies will be expanded to include other patterned structures, including prototypes of the silicon buried grating accelerator.

Construction of a Modular Sub-relativistic Electron Beam Test Station

We have designed and completed the vacuum system construction of a modular electron optic column for low-beta (up to 100keV energy incident) laser electron acceleration experiments. This modular system is designed for rapid prototyping and testing of various laser accelerator system components, including Ti:Sapphire laser driven fused silica and Tm:Fiber laser-driven silicon accelerator and deflector structures, and ultrafast

photocathode sources. The system currently uses a Kimball Physics 100keV LaB6 electron gun differentially pumped to $7x10^{-9}$ Torr, with additional beam focusing and scanning coils for SEM-style imaging and precise beam control, with a nanosecond beam blanker initially. The main chamber is held at $3x10^{-7}$ Torr for simplicity. The system will include a 6-axis motorized sample holder, 90 degree bending magnet spectrometer for acceleration monitoring, and a straight-through scintillator screen for deflection monitoring. It will enable both free-space laser coupling to the structure as well as fiber coupling via integrated optics, and allow multi-stage accelerator structures to be tested as well. The vacuum system is completed as of Q3 2013 (see Fig. 26), with the remainder of the system components expected to be completed in Q4 2013 and experiments beginning shortly thereafter. The modular design allows system components to be interchanged readily, for example replacing the Kimball Physics electron gun with a differentially pumped ultrafast photocathode source through our collaborations with SRI International and Peter Hommelhoff.

Figure 26: Completed low-beta electron column base system.

3. THREE-YEAR PLAN
(From 2010 proposal)

We propose to demonstrate the maximum accelerating gradient possible in laser-driven dielectric structures. This will be done in three steps. First, we will continue to develop our numerical simulation capabilities to accurately predict the outcome of the beam-based and bench-top experiments. This will be an iterative process where experimental results and understanding are used to improve the accuracy of the models. These models will then be used to design a 1 GeV laser-driven dielectric accelerator.

Second, we propose to conduct bench-top optical characterization of the structures. These experiments will include measurements of coupling, transmission, spectroscopy, mode identification, damage fluence, and the quality of structure fabrication for fibers, woodpile structures, and gratings.

Third, we propose to continue with the successful beam-based experiments at E163. The first of these will involve Schottky excited PBG fiber wakefield measurements, followed by net acceleration experiments similar to those reported in 2008. Additional wakefield and net acceleration experiments will be conducted for the woodpile structure and the gratings. Ultimately structures with integrated couplers will be tested.

The Three Year Plan in list format is shown below.

Year 1

1) Measure wakefield radiation from PBG fibers and compare with simulations
2) Power candidate photonic crystal fiber structure and IFEL at matched wavelength and perform first microstructure staging experiments, using simple free-space coupling
3) Fabricate woodpile structures and gratings.
4) Perform optical tests to benchmark design simulations
   a. Spectroscopy
   b. Coupling efficiency
   c. Mode identification
5) Explore material damage threshold
   a. Expand data to infrared spectrum out to 3 μm
   b. Look at additional promising materials and fully fabricated structures
6) Design couplers for fiber, woodpile, and grating structures

Year 2

1) Characterize optical properties of fibers, woodpile, and gratings
2) Conduct Beam-based measurements of fibers, woodpile and grating structures
   a. Wakefield radiation.
   b. Measurements of energy modulation and gain in optically powered woodpile and grating structures.
3) Test prototype couplers and begin fabrication of fully integrated structures with couplers.

4) Design focusing and steering elements for the woodpile and grating structure

Year 3

1) Design and fabricate structures with integrated power couplers.
2) Perform bench-top and beam-based measurements of fully integrated structures with couplers.
3) Evaluate the measured gradient in the various structures and develop a fully integrated design for a 1 GeV accelerator based on each of the candidate structures.
4) Begin to explore low beta (v<c) structures and electron sources.

We propose to conduct these studies in collaboration with the AARD group at SLAC. However, each item listed above is partially or fully funded by the LEAP grant, either through LEAP-funded nanofabrication facility fees, graduate student efforts, or software licenses. In the budget narrative that follows, more specific identification of what work is funded by this proposal will be discussed. The operating and maintenance costs associated with the accelerator-based structure tests are borne by SLAC. SLAC personnel are also involved in simulating, fabricating, and testing structures, and are not funded by this proposal. This proposal funds the design, simulation, and fabrication work of the named Stanford University participants, and also funds some significant capital equipment items needed for the experiments and simulations.

4. COLLABORATION EFFORTS

A. With industrial partners

Incom, Inc.

Our program with Incom has been ongoing for more than 5 years and is currently working on a Phase 1 SBIR from DOE. We have achieved 1 mm long cells with multi-defect structures that we have shown to support TM01 modes based on calculations of the complete structure with errors. This was constructed using borosilicate glass (BK-7) that we have tested in our damage studies. The Phase 2 program will focus on materials with high radiation tolerance, such as fused silica and quartz.

Tech-X

We are working closely with members from Tech-X in another Phase 1 SBIR related to woodpile structure simulations. The Phase 1 project is studying coupler designs and fabrication tolerances required for accelerator structures. We have been allotted time on the NERSC system to run these computationally demanding simulations.

B. Academic collaborations

Byer Group

The LEAP project has focused on a proof-of-principle demonstration for laser-driven particle acceleration. Development of laser technologies for future laser-driven particle accelerators has been a secondary emphasis. Prof. Byer's on-campus research efforts (funded by other grants) are centered on developing new types of lasers and advanced optics, often with objectives that have overlapped with our own. Our daily interaction and shared interests with these groups naturally leads to joint simple experiments that are synergistic and are an important starting point for long-term challenges that we will have to address. Two such efforts include laser phase locking and the application of fiber lasers to particle accelerators. Another is the radiation damage studies where the Cary and Hitachi spectrophotometers located in Ginzton Laboratories have proven indispensable for the radiation damage studies with gammas and neutrons.

In addition, the equipment and optics expertise on campus allows us to carry out characterization measurements (such as laser damage threshold for the particle accelerator structures) and also allows us to expeditiously construct and test devices (such as the TM*01 laser mode converter). The resources and expertise on campus have proven to be a valuable asset to the LEAP program and will continue to be in the future.

Harris Group

The Harris group at Stanford researches the growth, characterization, nanofabrication and device implementation of unique compound semiconductor materials. They have experience using carefully controlled molecular beam epitaxy (MBE) combined with nanolithography to prepare artificially structured materials with atomic layer control and enhanced performance. They recently became our collaborators and will focus on exploring novel materials with high damage threshold for dielectric acceleration applications.

Solgaard Group

The Solgaard group at Stanford focuses on the design and fabrication of micro-optical and nano-optical devices that combine MEMS, photonic crystals, integrated optics, and free-space optics. They recently began work on an alternative accelerator structure design that is based on the grating structure design but is made out of silicon to leverage their nanofabrication expertise with this material.

Dr. Peter Hommelhoff

Leader of the Ultrafast Quantum Optics Group at the Max Planck Institute for Quantum Optics. His group concentrates on laser-matter interaction on the (sub-) femtosecond time scale to conceive and realize new concepts to trap, guide and steer the electrons. He recently became our collaborator focusing on the development of electron source better suited to test our structures where electrons are emitted from sharp metal tips with the help of femtosecond laser pulses.

Prof. Minghao Qi

Associate Professor of Electrical and Computer Engineering at Purdue University. Prof. Qi has extensive experience in the field of nanotechnology, especially 3D nanofabrication and low-cost nanolithography; micro and nanophotonics, with emphasis on 3D photonic crystals and integrated Si photonic circuits. He recently became our collaborator focusing on the design of photonic structures for accelerator physics applications.

Dr. Gil Travish

Researcher at the Particle Beam Physics Laboratory (PBPL) in UCLA. He has worked in beam physics, radiation production and accelerator technology for the past 15 years including: the first high-gain FEL experiments (UCLA); first saturation of a visible high-gain FEL (ANL). In recent years he has began work on a Micro Accelerator Platform, a laser-driven optical-scale accelerator, as well as other dielectric-based accelerator-structures and studies. His group performs beam studies of their structures at the Next Linear Collider Test Accelerator (NLCTA) on SLAC site, with help of the E-163 experiment members.

Dr. Tomas Plettner

Researcher at KLA-Tencor. He obtained his Ph.D. under supervision of Prof. Byer. Dr. Plettner wrote the original paper on the grating accelerator structure and subsequent studies of geometry variations to obtain deflection and focusing grating structures, including a proposed undulator design and detailed analysis of the electromagnetic forces present in such structures.

Other resources at SLAC

In addition to our collaboration with the AARD group at SLAC, NLCTA personnel have played an important role in aiding us with the design of the E163 experiment and in training on and operation of the accelerator. In addition, extensive use of the on-site machine shop, cable shop, electronics group and vacuum group has been made for the construction of the E163 experiment site.

5. LIST OF CURRENT PARTICIPANTS

LEAP has been a collaboration between Stanford University and the AARD group at SLAC. Funding for the participants of Stanford was covered by the LEAP contract while funding for the AARD participants was covered by SLAC.

i. Principal investigator
R.L. Byer*

ii. SLAC Staff and postdocs, not funded by the LEAP contract
E. Colby, R. Noble , J. Spencer, D. Walz, R.J. England

iii. Graduate students
C. McGuinness, K. Soong, E. Peralta*, C. Rudy, B. Montazeri*, Stephen Wolf

iv. Other SLAC collaborators
S. Tantawi, C. Ng

v. Other Stanford collaborators, not funded by the LEAP contract
M. Diggonet, M. Fejer, J. Harris, M. Kasevich, O. Solgaard,

vi. Outside collaborators

Academic

James Rosenzweig	UCLA
Gil Travish	UCLA
Boris Kuhlmey	University of Sydney, Australia
Martin Wegener	University of Karlsruhe
Minghao Qi	Purdue University
Peter Hommelhoff	Max Planck Institute for Quantum Optics

Industry

Martin Fermann,	IMRA America, Inc
Liang Dong	IMRA America, Inc
Michael Minot	Incom, Inc.
Ben Cowan	Tech-X
Tomas Plettner	Independent Contractor

vii. Administrative Staff

R. Route*	Stanford

*Funded by the present LEAP 163 contract (DE-FG03-97ER41276).

COGNIZANT PERSONNEL

PRINCIPAL INVESTIGATOR: (For technical and scientific matters)

R. L. Byer
Edward L. Ginzton Laboratory
Stanford University
Stanford, California 94305-4088

Telephone: (650) 723-0226
FAX: (650) 723-2666
Electronic Mail: byer@stanford.edu

FOR ADMINISTRATIVE MATTERS: (Budgets, property, etc.)

Jennifer Wong
Edward L. Ginzton Laboratory
Stanford University
Stanford, California 94305-4088

Telephone: (650) 723-0184
FAX: (650) 725-8125
Electronic Mail: jrwong@stanford.edu

FOR CONTRACTUAL MATTERS: (Including overhead and patent questions)

Catherine Boxwell
Manager Contracts & Grants
Office of Sponsored Projects
3160 Porter Drive, Suite 100
Stanford University
Stanford, California 94304-8445

Telephone: (650) 725-6864
FAX: (650) 724-2290
Electronic Mail: boxwell@stanford.edu

6. BUDGET

Stanford Budget Justification

	8/1/2010 7/31/2011	8/1/2011 7/31/2012	8/1/2012 7/31/2013	TOTAL 3 YEARS
A. SALARIES AND WAGES[1]:				
R. L. Byer, The William R. Kenan Professor of Applied Physics and Principal Investigator, 1% effort for 3 Qtrs& 2% effort for 1 Qtr. each year; based on a full time rate $65,029 per Qtr. current year.	3,320	3,403	3,488	10,210
R. Route, Senior Research Engineer, 5% effort each month each year; based on a full time rate of $11,726 per month current year.	7,183	7,363	7,547	22,093
2 Graduate Research Assistant, 50% effort for 3 Qtrs. and 75% for 1 Qtr. each year; based on a full time rate of $16,086 per Qtr. current year.	73,907	75,755	77,649	227,311
Admin Associate 6% effort per month each year; based on a full time rate $5,213 per month current year.	3,832	3,928	4,026	11,786
SUBTOTAL SALARIES AND WAGES	88,242	90,448	92,710	271,400
B. STAFF BENEFITS: 30.6% of Faculty and Staff Salaries	4,387	4,496	4,609	13,491
5% of Graduate Research Assistant Salaries	3,695	3,788	3,882	11,366
C. EXPENDABLE MATERIALS AND SUPPLIES[2]:	40,700	34,300	43,750	118,750
D. TRAVEL[3]:	5,000	5,000	5,000	15,000
E. REPORTS AND PUBLICATIONS[4]:	1,250	1,250	1,250	3,750
SUBTOTAL: MODIFIED TOTAL DIRECT COST (MTDC)	143,274	139,282	151,201	433,757
F. INDIRECT COST: 60% of MTDC	85,965	83,569	90,720	260,254
G. CAPITAL EQUIPMENT[5]:	60,306	65,278	44,519	170,103
H. TUITION	40,455	41,870	43,560	125,885
TOTAL ESTIMATED COST	$330,000	$330,000	$330,000	$990,000

FOOTNOTES

1) SALARIES:
We anticipate that salaries will escalate at the rate of 2.5% each October 1st.The budgeted salary amount is comprised of the direct effort for the project plus 8.60% vacation accrual/disability sick leave (DSL) for employees and 7.20% for non-exempt employees. The above amounts do not exceed total salary. Vacation/DSL accrual will be charged at the time of the salary expenditure. No net salary will be charged when the employee is on vacation, disability or worker's compensation

2) EXPENDABLE MATERIAL AND SUPPLIES:

EXPENDABLES (includes the following)
Stanford Nanofabrication Facility, Capped at 2800 per month; variable access per year: 22,400, 16,000, 25,200
GL Micro Fab shop, $275 per month, each year: 3,300, 3,300, 3,300
Lab Supplies: 12,500, 12,500, 12,500
Computer software and maintenance: 1,000, 1,000, 1,000
Copying of research documents: 500, 500 750
General Office Supplies: 500, 500, 500
Shipping reports and apparatus: 500, 500, 320
Total: $40,700 $34,300 $43,570

3) TRAVEL:

1 person to Washington DC for program review each year:
Air fare, $650 each trip: 650, 650, 650
Per Diem, $125/day, 2 days each trip: 250, 250, 250
Ground Transportation: 100, 100, 100
Subtotal: $1,000, $1,000, $1,000

Two people to conference each year (PAC or AAC):
Round trip air fare, coach ($650) ea. Traveler: $1,300, $1,300, $1,300
5 day per diem ($250/day): 2500, 2500, 2500
Ground transportation, parking ($100) ea. Traveler: $200, 200, 200
Subtotal: $4,000, $4,000, $4,000
Travel Total: $5,000, $5,000, $5,000

4) REPORTS AND PUBLICATIONS:

Reports and publications include the annual technical publications of the research program and preparation charges for report materials. Page charges are in excess of $100 per page for the scientific journals we publish in.

5) CAPITAL EQUIPMENT:

Year 1

Fourier Transform Infrared Spectrometer (Thermo-fisher iN10 integrated FTIR microscope $55,200).
An FTIR will provide the ability to perform benchtop characterization of the photonic bandgap structures and assess the quality of the fabricated structure. This will also provide a measure of the frequency of the defect mode in fibers and other structures.
Total: 55,200*State Sales Tax (9.25%) 5,106 = $60,306

Year 2

(1) White-light Fiber source (Koheras model Super K red $24,551)
To effectively perform a variety of low power benchtop tests with proposed fiber accelerator structures with tunable radiation a white light fiber source will be necessary
(2) Photomultiplier Tube (Hamamatsu model R5509-73 ~$35,200).
The first set of wakefield experiments with the PBG fibers will be challenging due to the low photon yield. This PMT is a cooled unit providing better gain at longer wavelengths (out to 1700 nm) making it ideal for these types of measurements.
Total: 59,751 * State Sales Tax (9.25%) 5,527 = $65,278

Year 3

Gated camera (Roper Scientific model PI Acton PI-MAX2:1003HQ, $40,750)
This type image intensified camera was the most effective monitor for capturing the energy spectrum of the electron beam At E163 our anticipated run schedule will be too frequent to be able to borrow this camera from other experiments and we will require a dedicated camera.
Total: $40,750 * State Sales Tax (9.25%) 3,769 = $44,519

Personnel cost justification

1. **R.L. Byer, Principal Investigator.** Prof. Byer has initiated research on laser-driven particle acceleration and played a fundamental role in establishing the laser-electron accelerator project. As the principal investigator Prof. Byer oversees the general progress of research and establishes the main objectives of the program.

2. **R.K. Route, Senior Research Engineer.** Dr. Route manages the technical aspects of the program. These include coordination of purchases, salaries, and other laboratory expenses for this program with the university. In addition, Dr. Route is responsible for maintaining communication with the funding agency. Finally, Dr. Route assists the group with budget preparation, publications and report submissions.

3. **Postdoctoral Fellow.** A postdoctoral researcher brings expertise from outside the group and therefore can greatly enhance the pace at which progress takes place. We anticipate the ability to fund one postdoctoral fellow at the 50% level through this program. The postdoctoral fellow is expected to contribute in the laser and optics aspect of the program. The remaining 50% of the cost will be covered by the candidate's participation in other optics related programs in the Byer group. Other postdocs in the LEAP-E163 program are funded through SLAC.

4. **Graduate Student.** The LEAP-E163 program offers a wide range of research projects related to laser-driven particle acceleration that are well suited for thesis topics for graduate students. We plan to fund one graduate student through this program. Other students in the LEAP-E163 program are funded through SLAC.

5. **Administrative Associate.** The size of the LEAP-E163 project requires part-time assistance for the accounting management of the program.

6. **Engineering Technician.** A minor fraction of the equipment and vacuum components are maintained on campus, which requires part-time assistance from the campus-based engineering technician at the level of approximately 6 days per year.

7. BIOGRAPHIES

Robert L. Byer
Professor of Applied Physics, Stanford University

Education

Applied Physics, Stanford University, PhD	1969
Applied Physics, Stanford University, M.S.	1967
Physics, University of California, Berkeley	1964

Stanford University

Director, Edward L. Ginzton Laboratory, Stanford University	2006-2009
Director, Hansen Experimental Physics Laboratory, Stanford University	1997-2006
Co-Director, Stanford Photonics Research Center	2000-Present
Chair, Department of Applied Physics	2000-2002
Director, Center for Nonlinear Optical Materials, Stanford University	1992-2000
Dean of Research/Vice Provost, Stanford University	1987-1992
Associate Dean of Humanities and Sciences, Stanford University	1984-1986
Chair, Department of Applied Physics	1981-1984
Professor, Department of Applied Physics, Stanford University	1979-Present
Associate Professor, Department of Applied Physics, Stanford University	1974-1979
Assistant Professor, Department of Applied Physics, Stanford University	1969-1974
Employee, Spectra Physics Corporation	1964-1965

Professional Society Service

President, American Physical Society	2012-2013
Vice President, American Physical Society	2011-2012
Chair, California Council on Science and Technology	1995-1998
President, Optical Society of America	1994-1995
President, Lasers and Electro-Optics Society of the IEEE	1984-1985

Awards and Honors

Charter Fellow, National Academy of Inventors	2012
Frederic Ives Medal/Jarvis W. Quinn Prize, Optical Society of America	2009
Willis E Lamb Award for Laser Science & Quantum Optics, Physics of Quantum Electronics	2009
Photonics Award, Institute of Electrical and Electronics Engineers	2009
Distinction in Photonics Award, Spectra Photonics	2004
3rd Millennium Medal, Institute of Electrical and Electronics Engineers	2000
California Council on Science and Technology, Fellow	1999
A.L. Schawlow Award, Laser Institute of America	1998
R.W. Wood Prize, Optical Society of America	1998
Laser Institute of America, Fellow	1998
Quantum Electronics Award, Lasers and Electro-Optics Society	1996
American Association for the Advancement of Science, Fellow	1992
American Physical Society, Fellow	1992
R.V. Pole Memorial Lecture, Conference on Lasers and Electro-Optics	1987
Lasers and Electro-optics Society of the IEEE, Fellow	1987
Optical Society of America, Fellow	1976
Adolph Lomb Medal, Optical Society of America	1972
I.B.M., Fellow	1969

8. PUBLICATIONS

List of recent publications

A. Fiscal Year 2013

Refereed articles

1. E.A. Peralta, K. Soong, R.J. England, et al., "Demonstration of Electron Acceleration in a Laser-Driven Dielectric Microstructure," Nature, advance online publication, doi:10.1038/nature12664.
2. J. Breuer and P. Hommelhoff, "Laser-Based Acceleration of Nonrelativistic Electrons at a Dielectric Structure", Phys. Rev. Lett. 111, 134803 (2013)

Conference Proceedings

2013 Particle Accelerator Conference, Pasadena, CA

1. E. A. Peralta, et al., "High Gradient Acceleration of Electrons in a Laser-Driven Dielectric Micro-Structure," proceedings of the 2013 Particle Accelerator Conference, California (2013).
2. R. J. England, et al., "Applications for Optical-Scale Dielectric Laser Accelerators," proceedings of the 2013 Particle Accelerator Conference, California (2013).
3. K. Soong, et al., "Beam Position Monitor for Micro-Accelerators," proceedings of the 2013 Particle Accelerator Conference, California (2013).
4. Z. Wu, et al., "Silica Rod Array for Laser Driven Particle Acceleration," proceedings of the 2013 Particle Accelerator Conference, California (2013).
5. C. Lee, et al., "Fabrication of an 18 Layer 3D Photonic Crystal for Dielectric Laser Acceleration," proceedings of the 2013 Particle Accelerator Conference, California (2013).
6. C.K. Ng, et al., "Simulation of Power Coupling and Wakefield in Photonic Bandgap Fibers for Dielectric Laser Acceleration," proceedings of the 2013 Particle Accelerator Conference, California (2013).

B. Fiscal Year 2012

Refereed articles

1. T. Plettner, R. L. Byer, B. Montazeri, "Electromagnetic forces in the vacuum region of laser-driven layered grating structures," *Journal of Modern Optics*, vol. 58, issue 17, pp. 1518-1528 (2011).
2. K. Soong, R. L. Byer, "Design of a subnanometer resolution beam position monitor for dielectric laser accelerators," *Optics Letters*, Vol. 37, Issue 5, pp. 975-977 (2012).

Conference Proceedings

2012 Advance Accelerator Concepts Workshop, Austin, TX

3. R. J. England, et al., "Cherenkov Wakefield Excitation in Photonic Crystal Fiber Accelerators", to be presented at the 2012 Advance Accelerator Concepts Workshop (2012).
4. R. J. England, et al., "High Transformer Ratio Drive Beams for Wakefield Accelerator Studies", to be presented at the 2012 Advance Accelerator Concepts Workshop (2012).
5. E. A. Peralta, et al., "Design, Fabrication and Testing of a Fused-Silica Dual-Layer Grating structure for Direct Laser acceleration of electrons", to be presented at the 2012 Advance Accelerator Concepts Workshop (2012).
6. K. Soong, et al., "Laser Damage Threshold of Optical Materials for Dielectric Accelerators", to be presented at the 2012 Advance Accelerator Concepts Workshop (2012).
7. K. Soong, et al., "Diagnostic, Focusing, and Deflecting Dielectric Structures", to be presented at the 2012 Advance Accelerator Concepts Workshop (2012).
8. J. E. Spencer, et al., "Development of 2D PBG Structures for Accelerator Applications", to be presented at the 2012 Advance Accelerator Concepts Workshop (2012).
9. Z. Wu, et al., "Preliminary Results of the FACET Coherent Terahertz Radiation Source", to be presented at the 2012 Advance Accelerator Concepts Workshop (2012).
10. Z. Wu, et al., "Narrow Band Terahertz Radiation from e-Beam Driven Photonic Band Gap Structures", to be presented at the 2012 Advance Accelerator Concepts Workshop (2012).

C. Fiscal Year 2011

Refereed articles

7. C.K. Ng, R. J. England, L.-Q. Lee, R. Noble, V. Rawat, J. Spencer, "Transmission and radiation of an accelerating mode in a photonic band-gap fiber," *Phys. Rev. ST-AB* 13, 121301 (2010).
8. R. J. England, C.-K. Ng, R. J. Noble, and J. E. Spencer, "Input Coupler Design for Photonic Bandgap Fiber Accelerators," in preparation for submission to *Phys. Rev. ST-AB*.

Conference Proceedings

2011 Particle Accelerator Conference, New York, NY

9. K. Soong, et al., "Experimental Determination of Damage Threshold Characteristics of IR Compatible Optical Materials," proceedings of the 2011 Particle Accelerator Conference, New York (2011).
10. K. Soong, et al., "Simulation Studies of the Dielectric Grating as an Accelerating and Focusing Structure," proceedings of the 2011 Particle Accelerator Conference, New York (2011).
11. Z. Wu, C. Ng, C. McGuinness, and E. Colby, "Design of On-Chip Power Transport and Coupling Components for A Silicon Woodpile Accelerator", proceedings of the 2011 Particle Accelerator Conference, New York (2011).

12. Z. Wu, C. McGuinness, and E. Colby, "Terahertz Radiation Generation via e-Beam Driven Photonic Band Gap Structures", International Workshop on Optical Terahertz Science and Technology, Santa Barbara, Mar. 2011.
13. R. Laouar, E. Colby, R. J. England, R. Noble, “Measurement of Thermal dependencies of PBG Fiber Properties”, proceedings of the 2011 Particle Accelerator Conference, New York (2011).
14. R. J. England, E. R. Colby, R. Laouar, C. M. McGuinness, D. Mendez, C.-K. Ng, J. S. T. Ng, R. J. Noble, E. Peralta, K. Soong, J. E. Spencer, D. Walz, Z. Wu, D. Xu, "Experiment to Demonstrate Acceleration in Optical Photonic Bandgap Structures", invited talk, proceedings of the 2011 Particle Accelerator Conference, New York (2011).
15. Coupler Studies for PBG Fiber Accelerators J. Spencer, R.J. England, C.K. Ng, R. Noble, Z. Wu, Di Xu, proceedings of the 2011 Particle Accelerator Conference, also SLAC-PUB-14440, New York (2011).
16. C. McGuinness, et al., "Fabrication and Measurements of a Silicon Woodpile Accelerator Structure," proceedings of the 2011 Particle Accelerator Conference, New York (2011).
17. E. A. Peralta, et al, "Fabrication and Measurement of Dual Layer Silica Grating Structures for Direct Laser Acceleration, " proceedings of the 2011 Particle Accelerator Conference, New York.

9. CURRENT AND PENDING SUPPORT

ROBERT L. BYER

Name: Byer, Robert L. ACTIVE (SPO # 104774)
a. Source & Identifying No: National Science Foundation PHY-1068596
PI: Byer, Robert L.
Title: Stanford Program in support of LIGO
b. Your role on project: Principal Investigator
% Effort: 0.09 AY, .06 SMR
c. Dates and costs of entire project: 09/01/11 - 08/31/14
Directs: 2,839,390
Indirects: 1,360,610
d. Location: Stanford University

Name: Byer, Robert L. ACTIVE (SPO # 47080)
a. Source & Identifying No: California Institute of Technology 75ADV-1087852
PI: Byer, Robert L.
(Prime Sponsor: National Science Foundation)
Title: LIGO Project (Caltech) Support for the Seismic Isolation Subsystem
Cognizant Scientist for the Advanced LIGO Construction Project
b. Your role on project: Principal Investigator
% Effort: 1%, Academic Year, 0.09 per months
1%, Summer, 0.03 per months
c. Dates and costs of entire project: 09/01/09 – 03/31/14
Directs: 113,995
Indirects: 68,397
d. Location: Stanford University

Name: Byer, Robert L. ACTIVE (SPO # 47059)
a. Source & Identifying No: Department of the Navy N00014-10-1-0281
PI: Byer, Robert L.
Title: Novel Concept of Frequency-comb Interferometric Spectroscopy in the
Mid-IR for Significantly Enhanced Detection of Explosives
b. Your role on project: Principal Investigator
% Effort: 1%, Academic Year, 0.09 per months
7%, Summer, 0.21 per months
c. Dates and costs of entire project: 12/01/09 - 09/30/14
Directs: 691,900
Indirects: 297,787
d. Location: Stanford University

Name: Byer, Robert L. ACTIVE (SPO # 44768)
a. Source & Identifying No: National Aeronautics and Space Administration
NNX09AW13G

PI: Byer, Robert L.
Title: Laser Sensor for In-situ Detection of Chemical and Organic Biomarkers and Isotopes
b. Your role on project: Principal Investigator
% Effort: 5%, Academic Year, 0.45 per months
c. Dates and costs of entire project: 09/09/09 - 09/08/14
Directs: 868,734
Indirects: 300,147
d. Location: Stanford University

Name: Byer, Robert L. ACTIVE (SPO # 49740)
a. Source & Identifying No: Department of the Air Force FA95501010560
PI: Byer, Robert L.
Title: Research and Development of High Energy 2-micron Lasers Based on Tm: Doped Ceramic Laser Gain Media and Tm:
b. Your role on project: Principal Investigator
% Effort: 1%, Academic Year, 0.09 per months
10%, Summer, 0.30 per months
c. Dates and costs of entire project: 09/30/10 – 11/30/13
Directs: 1,255,107
Indirects: 544,893
d. Location: Stanford University

Name: Byer, Robert L. ACTIVE (SPO # 52514)
a. Source & Identifying No: DARPA N66001-11-1-4199
PI: Byer, Robert L.
Title: Laser-driven dielectric microstructure based advanced X-ray sources
b. Your role on project: Principal Investigator
% Effort: 1%, Academic Year, 0.09 per months
7.3%, Summer, 0.22 per months
c. Dates and costs of entire project: 09/30/11 - 09/29/14
Directs: 1,329,688
Indirects: 504,102
d. Location: Stanford University

Name: Byer, Robert L. PENDING (SPO # 107173)
a. Source & Identifying No: NASA
PI: Byer, Robert L.
Title: Test Mass Charge Control and Coating Enhancements for the LISA Gravitational Reference Sensor
b. Your role on project: Principal Investigator
% Effort: 1%, Academic Year, 0.09 per months
c. Dates and costs of entire project: 01/01/2013 - 12/31/2014
Total: 342,154
d. Location: Stanford University

Name: Byer, Robert L. PENDING (SPO # 109909)
a. Source & Identifying No: NASA
PI: Byer, Robert L.
Title: The drag-free CubeSat
b. Your role on project: Principal Investigator
% Effort: 3%, Summer, 0.09 per months
c. Dates and costs of entire project: 05/01//2013 - 04/30/2016
Total: 771,154
d. Location: Stanford University

Name: Byer, Robert L. PENDING (SPO # 111205)
a. Source & Identifying No: NASA
PI: Byer, Robert L.
Title: Ultra-quiet Inertial Reference Sensor
b. Your role on project: Principal Investigator
% Effort: 1%, Summer, 0.03 per months
c. Dates and costs of entire project: 10/01//2013 – 09/30/2015
Total: 55,835
d. Location: Stanford University

Name: Byer, Robert L. PENDING (SPO # 111906)
a. Source & Identifying No: NASA
PI: Byer, Robert L.
Title: Drag-free Control Systems for Small Satellites
b. Your role on project: Principal Investigator
% Effort: 3%, Summer, 0.09 per months
c. Dates and costs of entire project: 01/01/2014 – 12/31/2016
Total: 55,838
d. Location: Stanford University

10. REFERENCES

Introduction

1. M. Lenzner et al, “Femtosecond Optical Breakdown in Dielectrics”, Phys. Rev. Lett. 80, 4076 (1998)
2. Y.C. Huang, D. Zheng, W.M. Tulloch, R.L. Byer, “Proposed structure for a crossed-laser beam GeV per meter gradient, vacuum electron linear accelerator”, Applied Physics Letters, 68, no. 6, p 753-755 (1996)
3. Plettner, R.L. Byer, E. Colby, B. Cowan, C.M.S. Sears, J. E. Spencer, R.H. Siemann, “Proof-of-principle experiment for laser-driven acceleration of relativistic electrons in a semi-infinite vacuum”, Phys. Rev. ST Accel. Beams 8, 121301 (2005)
4. G. H. Kim et al. “Coupling of small, low-loss hexapole mode with photonic crystal slab waveguide mode,” Opt. Express 12, 6624–6631(2004)
5. B. Cowan, “Three-dimensional dielectric photonic crystal structures for laser-driven acceleration”, Phys. Rev. Accel. Beams, 11 011301 (2008).
6. C. McGuinness, et al, “Accelerating electrons with lasers and photonic crystals”, J. Modern Optics, 56 (18&19), p.2142ff, (2009).
7. X. E. Lin, “Photonic band gap fiber accelerator,” Phys. Rev. STAB 4, 051301(2001)
8. R. Noble, et al, “Designing photonic bandgap fibers for particle acceleration”, SLAC-PUB-12571, (2007).
9. A. Mizrahi and L. Schächter, “Optical Bragg accelerators”, Phys. Rev. E, 70, 016505, (2004).
10. B. Cowan, “Two-dimensional photonic crystal accelerator structures”, PRST-AB, 6, 101301, (2003).
11. T. Plettner et al “Proposed few-optical cycle laser–driven particle accelerator structure”, Phys. Rev. ST AB 9, 111301 (2006)

Progress During 2013

1. E.A. Peralta, K. Soong, R.J. England, et al., “Demonstration of electron acceleration in a laser-driven dielectric microstructure,” Nature, advance online publication, doi:10.1038/nature12664.
2. T. Plettner et al “Proposed few-optical cycle laser–driven particle accelerator structure”, Phys. Rev. ST AB 9, 111301 (2006).
3. K. Soong, R. L. Byer, Optics Letters, **37** 975 (2012).
4. Mizrahi and Schachter, "Optical Bragg Accelerators," PRE 70, 016505 (2004)
5. C. McGuinness, “Particle Accelerator on a Chip: Fabrication and Characterization of Woodpile Accelerator Structure.”Ph.D. thesis (Stanford University, 2012).
6. I. Staude, C. McGuinness, A. Frolich, R. L. Byer, E. Colby, and M. Wegener, Opt. Express 20, 5607-5612 (2012).